

# Network method for deformation analysis of three-dimensional point cloud with terrestrial laser scanning sensor

International Journal of Distributed  
Sensor Networks  
2018, Vol. 14(11)  
© The Author(s) 2018  
DOI: 10.1177/1550147718814139  
journals.sagepub.com/home/dsn  


Xiangyang Xu and Hao Yang 

## Abstract

The complexity of structural materials is increasing the importance of the technology for high accuracy measurement. How to obtain the displacement information of structural feature points accurately and efficiently is the key issue of deformation analysis. In this article, displacement analysis of a composite arched structure is investigated based on the terrestrial laser scanning technique. A new method based on the measured point cloud is proposed to analyze the displacement of surficial points, resulting in not only the displacement size but also the displacement direction. The innovation lies in extracting the displacement information with a network and remapped point cloud, which is called the network method. The displacement map obtained demonstrates that the transverse displacement in the experiment plays an important role in the safety of the structure, which could not be observed and obtained by the surface approximation method. Therefore, the panorama- and pointwise displacement analysis technologies contribute to ensure the safety of increasingly complex constructions.

## Keywords

Terrestrial laser scanning technology, deformation analysis, network method, point cloud data, pointwise displacement

Date received: 5 September 2018; accepted: 24 October 2018

Handling Editor: Francesc Pozo

## Introduction

High accuracy measurement is becoming increasingly important in the field of health monitoring considering the complexity of composite structures. How to obtain the displacement information of structural feature points accurately and efficiently is the key issue for structure deformation analysis. In this article, displacement of a composite arched structure is investigated based on a three-dimensional (3D) terrestrial laser scanning (TLS) technique. The structure deformation is analyzed by extracting the displacement information of network points with TLS surface-based scan characteristics. A network method (NM) based on a dense point cloud is proposed to extract the surficial point

displacement, with explicit displacement directions. The article is organized as follows. Section “Introduction” gives an introduction to the background and literature. Section “Experimental setup” describes the experiment setup and TLS measurement. The detailed steps of NM are introduced and performed in section “Data Analysis.” In section

---

Geodetic Institute, Faculty of Civil Engineering and Geodetic Science, Leibniz University Hannover, Hannover, Germany

### Corresponding author:

Hao Yang, Geodetic Institute, Faculty of Civil Engineering and Geodetic Science, Leibniz University Hannover, 30167 Hannover, Germany.  
Email: Yang@gih.uni-hannover.de



Creative Commons CC BY: This article is distributed under the terms of the Creative Commons Attribution 4.0 License

(<http://www.creativecommons.org/licenses/by/4.0/>) which permits any use, reproduction and distribution of the work without further permission provided the original work is attributed as specified on the SAGE and Open Access pages (<https://us.sagepub.com/en-us/nam/open-access-at-sage>).

“Discussion,” the displacement results of two epochs using the NM are illustrated and analyzed. Meanwhile, the displacement from the NM is compared with the surface approximation (SA) method and the accuracy is discussed. Finally, a conclusion is presented in section “Conclusion.”

### *TLS technology*

Traditional methods, which are limited to necessities of physical contact with the structures, restrict measurements to only the contact area and, thus, the amount of information regarding the deformation field is limited.<sup>1</sup> In the case of a higher complexity of mechanical behavior, it would be useful to have a larger amount of measurement data, where surface-based measurements or full-field measurements are dominant. Among the numerous surface-based measurement techniques available today, those applied in mechanical characterization include interferometry measurement, such as holographic interferometry (HI), digital speckle pattern interferometry (DSPI), digital holographic interferometry (DHI), and moiré interferometry (MI), which needs more complex experimental apparatuses, geometric moiré (MG) and grid methods (GM), which require surface treatment, such as the application of a grid onto the object’s surface for the measurements.<sup>2</sup>

The displacement information of certain critical points has an extremely important effect on the structural deformation in engineering projects, but these points are not convenient or suitable places to install the sensors and set the targets. In these situations, it is difficult to use traditional sensor technologies to achieve advantageous measurement results of some special parts of the structures, such as sharp corners, bulges, and depressions. Therefore, a new method is necessary and significant to analyze the displacement of feature points based on a surface-based point cloud. Several measurement technologies and corresponding analysis methods have been learned.<sup>3–5</sup>

TLS technology has been adopted extensively in many fields,<sup>6–12</sup> such as civil engineering, to understand and monitor the deformation of structures. It is commonly used to create 3D point clouds or digital elevation models to describe and characterize deformation behavior and better analyze and understand surface processes by comparing multiple acquisitions over time.<sup>13–16</sup>

### *Deformation analysis*

In this article, the deformation of the structure is analyzed by extracting the displacement of some important feature points. Feature extraction from point cloud data can be achieved automatically with the aid of two-dimensional projection and inverse transformation,

which are applied in, for example, 3D street views with enormous point cloud data.<sup>17</sup> However, this method requires the combined use of laser scanner, camera, position, and orientation systems and, thus, is not convenient to apply in single or local structures where the point cloud data are relatively small.

The TLS is an efficient technology for spatial information acquisition, which can determine a dense, 3D point cloud with fast, non-contact measurement.<sup>18</sup> Displacements were computed by a triangular mesh of the object’s surface and by the shortest distance between two surface models and applied in the deformation map of the dam.<sup>19</sup> The regular shape measured by TLS was computed by fitting lines and the vertical displacement is consistent with the traditional measurement of, for example, inductive transducers and leveling.<sup>20</sup> Displacement was obtained based on data co-registration<sup>21</sup> and a cross-correlation-based method.<sup>22</sup> The surface fitting method with moving least squares was used to derive a surface deformation field.<sup>23</sup>

Many kinds of measurement technologies are applied in the deformation analysis.<sup>24–26</sup> Vazquez<sup>27</sup> investigate the dynamic and semi-static displacement of a bridge with the GPS time series. Kibitkin et al.<sup>28</sup> analyzed the displacement vector fields and standard errors of deformation to choose the input parameters for the digital image correlation (DIC) method.

### **Experimental setup**

Experimentation was designed and carried out in close cooperation with structural engineers. An arched brick structure was constructed and equipped with load and testing equipment, aiming at the measurement and investigation of structural deformation behavior under vertical loads. The loads lasted continuously for 20 min each time (also named “epoch” subsequently) through four I-beams, which are beams with I-shaped cross sections. Measurements were carried out in the load pause of about 10 min. The arch structure was supported by two piers. With the increasing loads, the left pier was always stable with the ground, while the right one moved along the direction straight rightward. Some traditional measurements were set up by structural engineers, but, for the sake of detailed deformation information and surface-based results, the TLS measurement was conducted as presented in this article.

The TLS instrument adopted was the Z + F Imager 5006. It scans the surface of structures and records the surface information as a dense point cloud with coordinates in three dimensions and the intensity of a reflected laser. The scanning accuracy is 0.4 mm rms (root mean square) and the distance resolution is 0.1 mm with a sampling speed up to one million points per second. In the experiment, the TLS scanning time for a single

epoch is about 6 min and the point cloud density obtained is an average of 2 mm between neighboring points. Because of the complex setup of loading, the TLS scanner could only be positioned on a second floor to maintain optimal visibility of the main arch surface and have stable standpoint for itself. As a result, the point cloud data measured occurred as a blank due to the shadow of the I-beams, electrical wires, and so on. However, this would not influence the result of the analysis, since the polynomial surface involved is continuous and smooth globally, and the feature points to be extracted are not in the blank area.

The experiment setup is shown in Figure 1 from the standpoint of TLS measurement, where the white structures are the arch and two piers, and the load is applied from the top and distributed through four parallel I-beams in contact with the arch top surface. Absolute displacement analysis of net points is performed with the epoch data of TLS point clouds gathered experimentally.

Sheltering is unavoidable when the TLS laser propagation encounters obstacles. It can be observed in Figure 1 that the I-beams contact the arch surface from the top, which could shelter the laser beams. Therefore, the top surface forms blank areas, as shown in Figure 2.

## Data analysis

The introduction of the network aims at the displacement extraction in the surface area with explicit directions. This article proposes an NM to make full use of areal information and feature points for displacement analysis, where the point states in two epochs are compared at the exact points with a certain accuracy. The main principle lies in the construction of a reference network and the remapping of the point cloud. The reference network is constructed based on the processing of the local point cloud, where reducing the noises and uncertainties is highly emphasized.

The main steps of displacement extraction with the NM are described as follows. First, local stable planes are fitted on the stable reference object with TLS measurement. Stable points are extracted based on geometrical relations of the planes. Second, reference networks are constructed for the two pieces of measurement data for which the displacement is to be computed. Third, the arch point cloud is filtered iteratively to discard the outliers. Fourth, the point cloud is remapped according to the network and the point pairs are determined. Finally, the displacement is obtained with both size and direction information.

Construction of reference networks requires first and foremost stable objects. In the current experiment, the piers are considered as rigid bodies and, therefore,

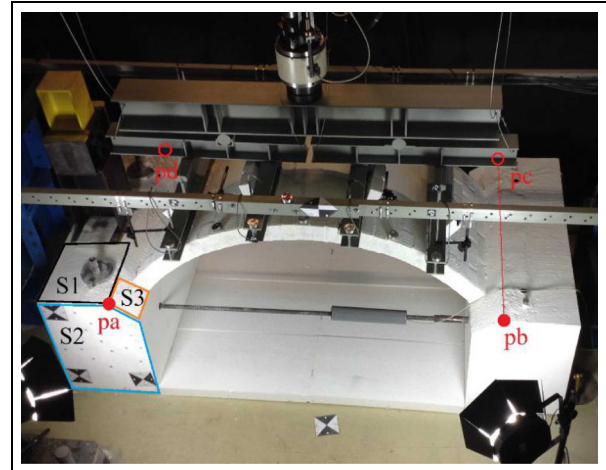


**Figure 1.** An arch experiment setup from the standpoint of TLS.

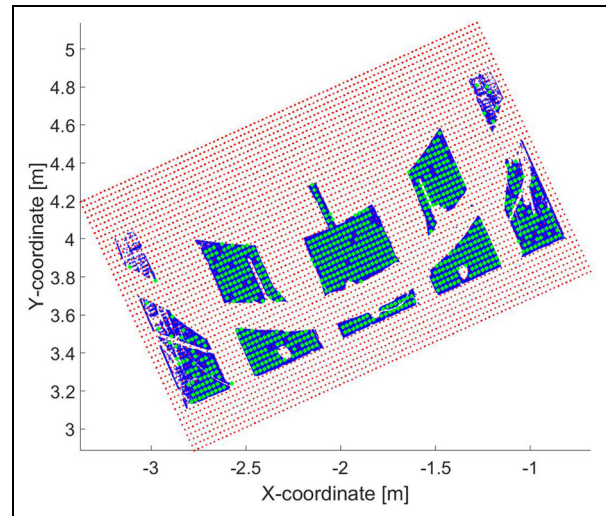


**Figure 2.** Network from the top view.

the features of the piers could be finalized to give the scans the same reference to compare scans captured at different times. Stable feature points are extracted with the aid of geometrical relations of a few high-quality planes on the piers, which are obtained by means of approximating TLS measurement data. The approximation of the point cloud is based on the least squares method and forms three planes, S1–3, as shown in Figure 1. The intersection of planes S1–3 generates point  $pa$  and  $pb$ , and the lines in the depth direction of the piers, marked as the lines connecting  $pb$  and  $pc$  in Figure 1. Considering the depth of the pier is generally stable and the direction of the depth is obtained as described above, the other two points  $pc$  and  $pd$  are determined uniquely given a depth of the pier of 1.5 m.

The network is constructed with the four stable points:  $pa$ ,  $pb$ ,  $pc$ , and  $pd$ . Equal-distance interpolation

is carried out on each side to form a network of size  $M \times N$  points where the length and width of the arch are divided into  $M = 100$  and  $N = 50$  equal parts, respectively. The network is shown in Figure 2 with red and green points. The blue points are the TLS measurement data of the arch top surface.

Attention is paid especially to the accuracy of the network construction. The approximation of planes S1–3 is repeated three times each to determine the most optimal solution for the planes. The accuracy is an average of 0.7 mm of the approximated planes S1–3. Because of plane characteristics, the approximated plane accuracy should approach the accuracy of the measurement points. The plane accuracy result agrees with measurement uncertainty from the work by Wujanz et al.<sup>29</sup> as  $0.68 \pm 0.05$  mm, computing with the laser intensity value. The uncertainty could come from the TLS measurement uncertainty and, additionally, the properties of the surface measured. Nevertheless, the submillimeter accuracy is acceptable for the detection of large deformations, especially for the later epochs in this experiment, while the method could also give valuable references for the early epochs.

The point cloud data in Figure 2 are preprocessed with polynomial approximation, so that the points with errors larger than three times standard deviation (SD) are discarded. The complexity of the polynomial surface is determined by model testing, where the fourth-order polynomial with 15 parameters is chosen. Iterative filtering is carried out, where, finally, the SD is under 2 mm after five iterations. The accuracy of the point cloud should be improved for further research, for example, with preknowledge of the object shapes.<sup>30</sup>

The network is a reference to the point cloud data measured. Because the  $M$  and  $N$  values are, respectively, the same in two epochs, point pairs are generated in the two epochs at each net point where the index is absolutely the same, written as  $(i, j)$  with  $i \leq M$  and  $j \geq N$ . The two epochs are connected through reference networks constructed with the same stable points in two epochs.

It could be observed in Figure 2 that the network encircles the top surface of the arch, where the point cloud could be remapped to the network, similar to pixels. The cloud points are matched to the net points by means of nearest neighbor search based on the  $k$ -dimensional tree method, where the points as close as a distance threshold of 1 mm to the net points are recorded. The distance threshold is chosen depending on the requirement of the data processing. On one hand, a small threshold leads to fewer cloud points matched to the network and, thereafter, fewer point data for displacement analysis; on the other hand, a large threshold results in more points remaining, but the latter could not represent the position of the net points reliably.

The green points in Figure 2 correspond to the positions of remapped measurement points and the matched net points. With the remapped point cloud, we manage to calculate the spatial displacement of each point. Because the matched net point pairs own the same index in two epochs, the epochal deviation of the one-by-one remapped measurement points, that is, the 3D displacement, is obtained under the same index.

## Discussion

The displacements of the remapped point cloud are finally obtained by the NM, which could reflect the areal deformation behavior and the explicit displacement directions. The displacement vectors of two epochs are shown in Figure 3 from the lateral view, where Figure 3(a) depicts the displacement of an early epoch,  $E_3$ , corresponding to a small load, and Figure 3(b) describes the displacement of a later epoch,  $E_{13}$ , with a large load. The  $E_3$  (with load 120 kN) is a typical term without crack and  $E_{13}$  (520 kN) stands for a stage with crack.

The detailed displacement analysis is performed due to the explicit result of the pointwise displacement. It could be observed in Figure 3 that the structure behaviors vary in different parts of the arch in the early and late epochs. In the middle part of the arch, Figure 3(a) shows a much smaller displacement than Figure 3(b), while both displacement directions are almost vertical, as shown in the  $B_1$  and  $B_2$  areas of Figure 3. The displacement is increasing for the part of the arch close to the fixed left pier, but the direction changes from down left (as in area  $A_1$ ) to approximately vertical (as in area  $A_2$ ). This agrees with the fact that the shape of the arch increases the bearing capability of the structure, since the load is diverted in the horizontal plane and, thus, the vertical aspect is protected. However, after the load has increased greatly, the protection mechanism disappears, and the displacement direction turns to the vertical direction correspondingly. For the area of the right part of the arch, the direction of the displacement changes from up left (area  $C_1$ ) to mainly up (area  $C_2$ ), and the displacement size becomes smaller. This interesting phenomenon is caused by the fact that the right supporting pier is moving to the right during the loading process.

The accuracy of NM feature displacement is discussed through comparison with polynomial deformation. The fourth-order polynomial surface is approximated and the vertical displacement of the points referred to is computed. The difference of the displacement with two methods is shown in Figure 4, where the blue polyline corresponds to the displacement with NM and the red polyline refers to the polynomial surface.

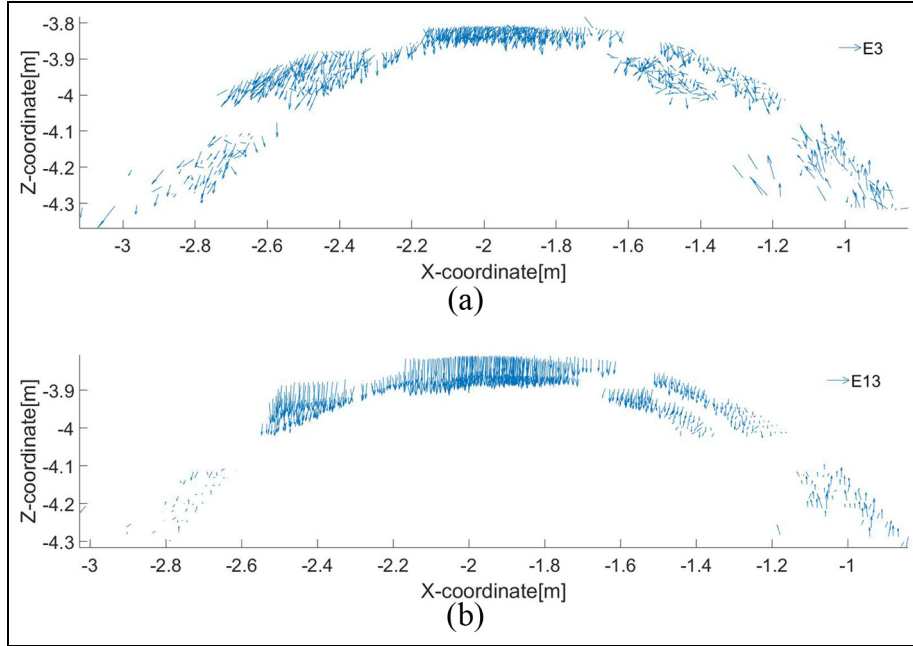


Figure 3. Spatial displacement with NM: displacement distribution of (a) E3 and (b) E13.

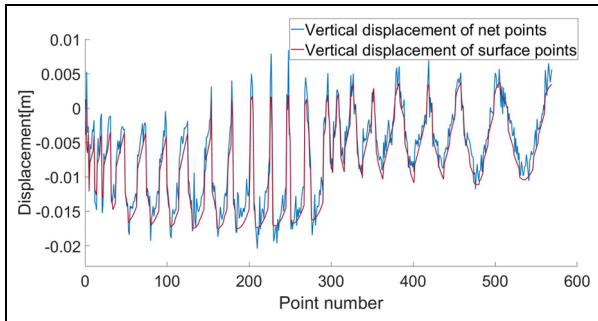


Figure 4. Difference of NM and SA in vertical displacement.

It could be observed in Figure 4 that the displacement trend of NM agrees well with the SA method. The NM displacement shows more details and the SA method gives only rough results. This is because it is possible to filter some important features using the SA method, which could be important for the description of displacement behaviors. Table 1 shows the mean value and SD of the vertical displacement of the NM and SA method. It is illustrated that the results are very close to each other and the difference is around 1 mm.

The NM gives extra results in the X and Y directions compared to the SA method, which offers displacement in the Z direction. Comparison is made and shown in Figure 5, where the blue polyline shows the difference between the displacement of the SA and the vertical direction displacement of the NM, and the red polyline corresponds to the deviation of the displacement of the SA and the 3D displacement of the NM. It is

Table 1. Comparison of vertical displacement of NM and SA.

Vertical displacement (mm)	E <sub>3</sub>		E <sub>13</sub>	
	Mean	SD	Mean	SD
NM	-1.07	1.46	-6.75	6.37
SA	-1.34	0.96	-8.07	6.25
Difference	0.27	0.50	1.32	0.12

NM: network method; SA: surface approximation; SD: standard deviation.

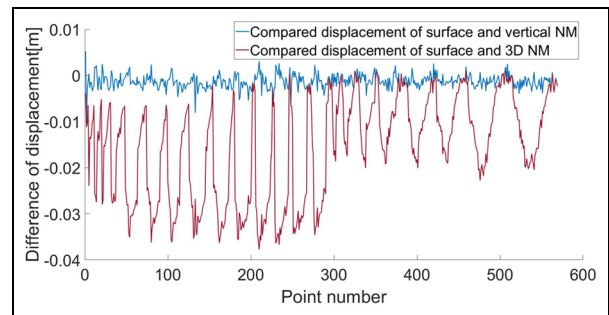


Figure 5. Comparison on NM and SA of 3D and vertical displacement.

demonstrated in Figure 5 that the vertical direction displacement of the NM approaches the displacement of the SA, while the 3D displacement of the NM is larger than the displacement of SA due to the displacement in the X and Y directions. The corresponding mean differences are listed in Table 2.

**Table 2.** Difference of the NM and SA displacement.

Mean difference (mm)	$E_3$	$E_{13}$
NM vertical vs SA	0.27	1.32
NM 3D vs SA	3.41	15.90

NM: network method; SA: surface approximation; SD: standard deviation.

The mean difference is computed by the NM value, subtracting the SA value and averaging. It is shown in Table 2 that the mean differences between the NM vertical displacement and the SA displacement are around 1 mm in both epochs, while the mean difference between the NM 3D displacement and the SA displacement is significantly larger. It is hinted that the NM result is point-to-point displacement, which offers extra displacement information in the X and Y directions and possibly contains the points which are significantly deformed but filtered by SA.

## Conclusion

In this article, TLS measurements were carried out for a structure load experiment to investigate the deformation behavior of an arched structure. A new method is proposed to obtain the displacement information of structural surficial points efficiently, where not only the displacement size but also the displacement direction could be successfully acquired. A network is constructed with stable objects and the point cloud is remapped according to the network. The remapped points are extracted and the deviations with different epoch data are calculated.

Accuracy of the network is highly emphasized, where multi-tries are performed to generate a reliable reference network. The fitted planes obtained an accuracy under 1 mm. The arch point cloud was filtered with optimal polynomials, where the outliers are discarded with five iterations and the uncertainty is under 2 mm, to improve the displacement result.

It is shown that the transverse displacement in the experiment plays an important role in the safety of the structure. Therefore, it is not sufficient to assess the health of structures based solely on vertical displacements, which is one shortcoming of SA assessment methods. Therefore, a panorama- and surface-based monitoring technology is required to ensure the safety of increasingly complex constructions.

## Acknowledgements

The authors wish to acknowledge the support of all the colleagues in Geodetic Institute of Leibniz University Hannover for their valid information.

## Declaration of conflicting interests

The author(s) declared no potential conflicts of interest with respect to the research, authorship, and/or publication of this article.

## Funding

The author(s) disclosed receipt of the following financial support for the research, authorship, and/or publication of this article: The publication of this article was funded by the Open Access Fund of the Leibniz Universität Hannover and also supported by Natural Science Foundation of Jiangsu Province (no. BK20160558).

## ORCID iD

Hao Yang  <https://orcid.org/0000-0001-7883-9808>

## References

1. Liu W, Chen SE, Boyajian D, et al. Application of 3D LiDAR scan of a bridge under static load testing. *Mater Eval* 2010; 68(12): 1359–1367.
2. Bruno L. Mechanical characterization of composite materials by optical techniques: a review. *Opt Laser Eng* 2018; 104: 192–203.
3. Yang H, Xu X and Neumann I. Deformation behavior analysis of composite structures under monotonic loads based on terrestrial laser scanning technology. *Compos Struct* 2018; 183: 594–599.
4. Xu X, Yang H and Neumann I. A feature extraction method for deformation analysis of large-scale composite structures based on TLS measurement. *Compos Struct* 2018; 184: 591–596.
5. Yang H, Omidalizarandi M, Xu X, et al. Terrestrial laser scanning technology for deformation monitoring and surface modeling of arch structures. *Compos Struct* 2017; 169: 173–179.
6. Yang H, Xu X and Neumann I. Laser scanning-based updating of a finite-element model for structural health monitoring. *IEEE Sens* 2016; 2100–2104.
7. Xu X, Zhao X, Yang H, et al. TLS-based feature extraction and 3D modeling for arch structures. *J Sens* 2017; 17: 9124254.
8. Yang H, Xu X and Neumann I. Optimal finite element model with response surface methodology for concrete structures based on terrestrial laser scanning technology. *Compos Struct* 2018; 183: 2–6.
9. Ko C, Sohn G, Rimmel TK, et al. Maximizing the diversity of ensemble random forests for tree genera classification using high density LiDAR data. *Remote Sens* 2016; 8: 646.
10. Yang H, Xu X, Xu W, et al. Terrestrial laser scanning-based deformation analysis for arch and beam structures. *IEEE Sens J* 2017; 17: 4605–4611.
11. Yang H, Xu X and Neumann I. The benefit of 3D laser scanning technology in the generation and calibration of FEM models for health assessment of concrete structures. *Sensors* 2014; 14: 21889–21904.
12. Xu X, Kargoll B, Bureick J, et al. TLS-based profile model analysis of major composite structures with robust B-spline method. *Compos Struct* 2018; 184: 814–820.

13. Eitel JUH, Höfle B, Vierling LA, et al. Beyond 3-D: the new spectrum of LiDAR applications for earth and ecological sciences. *Remote Sens Environ* 2016; 186: 372–392.
14. Villarino A, Riveiro B, Martínez-Sánchez J, et al. Successful applications of geotechnologies for the evaluation of road infrastructures. *Remote Sens* 2014; 6: 7800–7818.
15. Jung J, Chen L, Sohn G, et al. Multi-range conditional random field for classifying railway electrification system objects using mobile laser scanning data. *Remote Sens* 2016; 8: 1008.
16. Ko C, Sohn G, Rimmel TK, et al. Hybrid ensemble classification of tree genera using airborne LiDAR data. *Remote Sens* 2014; 6: 11225–11243.
17. Li Y, Hu Q, Wu M, et al. Extraction and simplification of building façade pieces from mobile laser scanner point clouds for 3D street view services. *ISPRS Int J Geo Inf* 2016; 5: 231.
18. Walton G, Delaloye D and Diederichs MS. Development of an elliptical fitting algorithm to improve change detection capabilities with applications for deformation monitoring in circular tunnels and shafts. *Tunn Undergr Sp Tech* 2014; 43: 336–349.
19. Alba M, Fregonese L, Prandi F, et al. Structural monitoring of a large dam by terrestrial laser scanning. *Int Arch Photo Remote Sens Spat Inform Sci* 2006; 36: 1–6.
20. Lovas T, Barsi A, Detrekoi A, et al. Terrestrial laser scanning in deformation measurements of structures. *Int Arch Photo Remote Sens Spat Inform Sci* 2008; 37: 527–532.
21. Aryal A, Brooks BA, Reid ME, et al. Displacement fields from point cloud data: application of particle imaging velocimetry to landslide geodesy. *J Geophys Res* 2012; 117: F01029.
22. Qin R, Tian J and Reinartz P. 3D change detection—approaches and applications. *ISPRS J Photogramm* 2016; 122: 41–56.
23. Li J, Wan Y and Gao X. A new approach for subway tunnel deformation monitoring: high-resolution terrestrial laser scanning. *Int Arch Photo Remote Sens Spat Inform Sci* 2012; 39: 223–228.
24. Villarino A, Riveiro B, Gonzalez-Aguilera D, et al. The integration of geotechnologies in the evaluation of a wine cellar structure through the finite element method. *Remote Sens* 2014; 6: 11107–11126.
25. Xu X, Yang H, Zhang Y, et al. Intelligent 3D data extraction method for deformation analysis of composite structures. *Compos Struct* 2018; 203: 254–258.
26. Raunonen P, Kaasalainen M, Akerblom M, et al. Fast automatic precision tree models from terrestrial laser scanner data. *Remote Sens* 2013; 5: 491–520.
27. Vazquez GE, Gaxiola-Camacho JR, Bennett R, et al. Structural evaluation of dynamic and semi-static displacements of the Juarez Bridge using GPS technology. *Measurement* 2017; 110: 146–153.
28. Kibitkin V, Solodushkin A, Pleshanov V, et al. On a choice of input parameters for calculation the vector field and deformation with DIC. *Measurement* 2017; 95: 266–272.
29. Wujanz D, Burger M, Mettenleiter M, et al. An intensity-based stochastic model for terrestrial laser scanners. *ISPRS J Photogram* 2017; 125: 146–155.
30. Xu X, Yang H and Neumann I. Time-efficient filtering method for three-dimensional point clouds data of tunnel structures. *Adv Mech Eng* 2018; 10(5): 1–6.